CoMFA and CoMSIA on the Neuroblocking Activity of 1-(6-Chloro-3-pyridylmethyl)-2-nitroiminoimidazolidine Analogues

Nack-Do Sung,* Seok-Chan Jang, and Kyoung-Seop Choi

*Division of Applied Biology & Chemistry, College of Agriculture and Life Sciences, Chungnam National University, Daejeon 305-764, Korea. *E-mail: ndsung@cnu.ac.kr*
Received July 5, 2006

3D-QSARs on the neuroblocking activities by 1-(6-chloro-3-pyridylmethyl)-2-nitroiminoimidazolidine analogues as agonist at the nicotinic acetylcholine receptor (nAChR) were studied quantitatively using CoMFA and CoMSIA methodologies. The statistical results of CoMFA (A5: $r^2_{cv.} = 0.707$ & $r^2_{ncv.} = 0.986$) and CoMSIA model (A3: $r^2_{cv.} = 0.715$ & $r^2_{ncv.} = 0.961$) showed the best predictability and fitness for neuroblocking activity based on the cross-validated value and non-cross validated value. The steric and H-bond acceptor nature of a compound were essential for high activity. The study on 3D-QSARs between substrate molecules and their neuroblocking activities appears to be an useful approach for designing better neuroblocking drug development.

Key Words : Imidacloprid analogues, Neuroblocking activity, CoMFA, CoMSIA analysis

Introduction

1-(6-Chloro-3-pyridylmethyl)-2-nitroiminoimidazolidine (common: Imidacloprid)[1] analogues are a class of insecticides that acts selectively on insect neuronal nicotinic acetylcholine receptors (nAChRs) (*i.e.* neonicotinoid insecticide) is used widely to protect crop and control pest.[2] In mammals, nAChR agonists have been shown to improve performance in a variety of memory tasks, whereas treatment with nAChR antagonists has been shown to impair memory functions.[3] The nAChRs exist as various subtypes and are involved in a variety of functions and disorders of the central nervous system, such as Alzheimer and Parkinson diseases.

Recently, imidaclopride analogues were evaluated and investigated to study on seed treatment,[4] uptake and persistence,[5] soil functioning,[6] an enzyme-linked immunosorbent assay (ELISA),[7] specific nicotinic agonist[8] and insecticidal neuroblocking,[9] proboscis extension response (PER) assay,[10] quantifying imidaclopride and it's metabolite,[11] cytogenic and genotoxic effects[12] of neonicotinoids. And also the nicotinic potency of many neonicotinoids have been characterized to examine the quantitative structure-activity relationships (QSARs).[13] Studies on structure-affinity relationships (SAFIRs) of nAChR agonists have been reported.[14] To control the residual toxicity with half-life and design of new drug from transition-state mimic, it was reported previously that the hydrolysis of imidacloprid proceeds through the nucleophilic addition-elimination mechanism from kinetics data.[15]

In this report, to find the necessary information for drug design, comparative molecular field anaylsis (CoMFA)[16] and comparative molecular similarity indices analysis (CoMSIA)[17] were carried out to study three dimensional quantitative structure-activity relationships (3D-QSAR)[18] between neuroblocking activities and 1-(6-chloro-3-pyridylmethyl)-2-nitroiminoimidazolidine analogues which is substituted at 5-position.

Materials and Methods

Molecular Modeling. The neuroblocking activities (log1/BC) of 1-(5-(X) substituted-6-chloro-3-pyridylmethyl)-2-nitroiminoimdazolidine analogues (**1-21**) as agonist at the

Table 1. Observed neuroblocking activities, Obs.log(1/BC) of imidacloprid analogues and predicted activities by 3D-QSAR models

No.	Sub. (X)	Obs.	CoMFA		CoMSIA	
			Pred.	Dev.	Pred.	Dev.
2	F	5.99	5.94	0.05	5.68	0.31
3	Cl	5.61	5.52	0.09	5.61	0.00
4	Br	5.51	5.50	0.01	5.58	–0.07
5	I	5.30	5.31	–0.01	5.54	–0.24
6	CH_3O	4.98	4.50	0.48	5.04	–0.06
7	C_2H_5O	4.66	4.54	0.12	4.73	–0.07
9	*i*-C_3H_7O	4.46	4.40	0.06	4.53	–0.07
11	*n*-$C_5H_{11}O$	3.59	3.63	–0.04	3.54	0.05
12	CH_3	5.25	5.43	–0.18	5.12	0.13
14	*n*-C_3H_7	4.51	4.50	0.01	4.41	0.10
15	*n*-C_4H_9	3.79	3.77	0.02	3.94	–0.15
16	C_6H_5	4.46	4.56	–0.10	4.33	0.13
17	CF_3	4.43	4.38	0.05	4.54	–0.11
18	CO_2CH_3	3.92	3.92	0.00	3.87	0.05
19	CN	4.59	4.71	–0.12	4.50	0.09
21	N_3	4.98	4.99	–0.01	5.07	–0.09
	ARTS			0.08		0.11
	PRESS			0.32		0.27

Pred.; predicted values by the optimized CoMFA model (A5) in Table 2 and CoMSIA model (A3) in Table 3, Dev.; different between observed and predicted value, ARTS; average residual of training set, PRESS; redictive residual sum of squares of the training set.

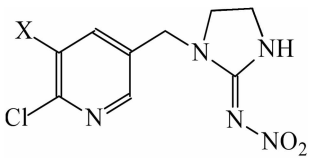

Figure 1. General structure of 1-(6-chloro-3-pyridylmethyl)-2-nitroiminoimdazolidine analogues (**1-21**).

nicotinic acetylcholine receptor (nAChR) were taken from the literature[19] and their activities are listed in Table 1. And Figure 1 represents the general structure of imidacloprid analogues employed in this study. Molecular field calculations and partial least-squares (PLS) analyses have been performed using the CoMFA and CoMSIA modules within SYBYL package (Version 7.1).[20] The structures of imidacloprid analogues were energy-minimized using the SYBYL energy minimizer (Tripos Force Field) with a 0.01 kcal/mol energy gradient convergence criterion and Gästeiger-Hückel charge.[21] The lowest energy conformation was searched with simulated annealing method.[22] Both CoMFA and CoMSIA models were obtained with 16 molecules in training set and 5 molecules in test set. The compounds of training set were aligned in 3 dimensional space by atom based fit (A)[23] and field fit (F)[24] with alignment rule. For an example, one of the two alignments for training set, the atom based fit, is shown in Figure 2. And the CoMFA combined with hydrophobic interaction (HINT) analysis[25] were carried out using the QSAR module of SYBYL package.

Region Focusing. This is usually applied to enhance the predictability of a CoMFA and CoMSIA study. Region focusing is the weight application to the lattice points within a CoMFA and CoMSIA region to enhance or attenuate the contribution of those points for subsequent analysis.[20] StDev*Coefficient values were used as weights, and among different weighting factors were applied in that 0.5 was found as most appropriate. To improve the predictability of the CoMFA and CoMSIA models, region focusing was attempted. According to the reference,[26] a model improvement should only be trusted if the q^2 value increases as much as 10%.

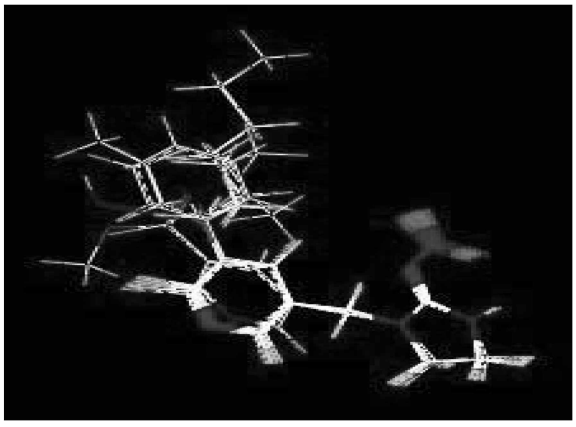

Figure 2. Alignment of the potential energy minimized agonists according to a least-squares atom based fit.

Partial Least Square (PLS) Analysis. This method was used to linearly correlate the activities with the CoMFA and CoMSIA values. To avoid over-fitted 3D-QSAR, the optimum number of components used in the model derivation is chosen from the analysis with the highest cross-validated correlation coefficient, r^2_{cv} (or q^2). 3D-QSAR method can avoid some inherent deficiencies arising from the functional form of Lennard-Jones and Coulomb potentials. Moreover, the contour maps of the relative spatial contributions in the different fields can be substantially improved, which is very intuitive for interpretation in terms of separate property fields.[27] The cross-validated q^2 quantifies the predictive ability of the model. It was determined by a leave-one-out (LOO) procedure of cross-validation in which one compound is removed from the dataset and its activity is predicted using the model derived from the rest of the data set. After the predictive quality of the best correlation model is determined, the optimum number of component is employed to do no validation PLS analysis in order to get the final model parameters such as correlation coefficient (r^2), standard error of estimate (SEE) and F value.

Calculation of 3D-QSAR Descriptors. CoMFA and CoMSIA were performed with the QSAR option of SYBYL.[20] For all steps of conventional CoMFA, the default SYBYL settings were used. The steric (S) and electrostatic (E) field energies were calculated using the Lennard-Jones potential and Coulomb potential (sp^3 carbon probe atoms with +1 charge). Also, potential atomic charges were calculated using Gästeiger-Hückel method. CoMFA grid spacing used in this work was 1.0-3.0 Å in all X, Y and Z directions. In addition to the fields used in CoMFA method, the CoMSIA method provides hydrophobic (H), H-bond donor (D) and H-bond acceptor (A) fields.[28] Grid spacing used in this work was 1.0-3.0Å which is same as shown in CoMFA study. A probe atom with radius 1.0 Å, hydrophobicity of +1.0 charge and H-bond properties (donor and acceptor) of +1.0 was used to calculate steric, electrostatic, hydrophobic, and H-bond fields, respectively.

Results and Discussion

Activities and Predictivity of the Models. The observed neuroblocking activity (*Obs.*log(1/BC)) of imidacloprid analogues (**1-21**) along with predicted activity (*Pred.*log.(1/BC)) by CoMFA (A5) and CoMSIA models (A3), and the deviation (Dev.) of the predicted values from the observed values are summarized in Table 1. The neuroblocking activities of halogen substituents (**2-5**) were higher than those for compounds having any other group at the corresponding 5-position on pyridine ring. When the alkyl and alkoxy substituents with steric bulky groups were introduced as X-substituents, they showed little activities.

The results of CoMFA and CoMSIA analyses were summarized in Tables 2 and 3, respectively. The quality of the final optimized CoMFA and CoMSIA model is measured by two statistical parameters, r^2_{ncv} and q^2 (or r^2_{cv}). The value of q^2, which indicates the quantified predictability of

Table 2. The summary of statistical results of CoMFA models[a] with two alignment types and field contribution (%)

Alignments	Atom based fit					Field fit				
Models No.	A1	A2	A3	A4	A5[e]	F1	F2	F3	F4	F5
Fields combination	S	I	SI	SH	SIH	S	I	SI	SH	SIH
Grid (Å)	2.5	1.5	2.5	2.5	2.5	2.5	1.0	1.0	1.0	1.0
Component	4	4	4	4	4	3	4	3	3	3
$r^2_{cv.}$[b]	0.668	0.557	0.703	0.694	0.707	0.637	0.545	0.640	0.600	0.666
$r^2_{ncv.}$[c]	0.984	0.986	0.963	0.986	0.986	0.863	0.963	0.903	0.906	0.958
SEE[d]	0.101	0.095	0.152	0.093	0.092	0.279	0.153	0.235	0.231	0.155
F-value	165.844	187.785	71.640	194.962	200.631	25.253	70.659	37.176	38.659	90.562
Steric	56.1	91.0	66.3	67.6	76.4	53.1	93.1	57.5	47.5	61.3
Electrostatic	40.5	0.0	36.0	27.4	21.9	40.1	4.4	41.8	37.2	33.6
Hydrophobicity	3.3	9.0	3.7	4.9	1.7	6.8	2.5	0.7	15.3	5.1

Abbreviation: S = standard, I = indicator, H = H-bond field, [a]weight by StDev*Coefficient region focusing, [b]cross-validated $r^2_{cv.}$, [c]non-cross-validated $r^2_{ncv.}$, [d]standard error estimate, [e]the optimized model.

Table 3. The summary of statistical results of CoMSIA models[a] with two alignment types and field contribution (%)

Alignments	Atom based fit					Field fit				
Models No.	A1	A2	A3[e]	A4	A5	F1	F2	F3	F4	F5
Fields combination	SD	SA	SDA	SEAD	SHDA	SD	SHA	SDA	SEAD	SHDA
Grid (Å)	1.0	1.5	1.5	1.5	3.0	1.0	3.0	2.5	1.5	3.0
Component	4	2	4	3	2	3	2	2	3	2
$r^2_{cv.}$[b]	0.779	0.763	0.715	0.603	0.650	0.751	0.685	0.750	0.638	0.696
$r^2_{ncv.}$[c]	0.904	0.906	0.961	0.881	0.899	0.901	0.845	0.854	0.887	0.851
SEE[d]	0.244	0.222	0.157	0.260	0.231	0.237	0.285	0.277	0.254	0.280
F-value	25.883	62.678	66.926	29.614	57.568	36.404	35.568	38.807	31.298	37.160
Steric	94.6	67.8	68.2	54.8	52.2	82.5	45.1	61.3	54.8	44.1
Electrostatic	–	–	–	30.2	–	–	–	–	22.3	–
Hydrophobicity	–	–	–	–	27.8	–	38.4	–	–	37.6
H-bond Donor	5.4	–	0.8	0.5	0.7	17.5	–	5.2	2.6	4.3
H-bond Acceptor	–	32.2	31.0	14.5	19.4	–	16.5	33.4	20.3	14.0

Abbreviation: S = steric, E = electrostatic, H = Hydrophobicity, D = H-bond donor, A = H-bond, acceptor, [a]weight by StDev*Coefficient region focusing, [b]cross-validated $r^2_{cv.}$, [c]non-cross- validated $r^2_{ncv.}$, [d]standard error estimate, [e]the optimized model (α = 0.3).

the model, should be greater than 0.50 and the value of $r^2_{ncv.}$, which shows the self consistency of the model, should be greater than 0.90. And PRESS is the prediction error sum of squares. From the Table 1, it was found that the two models showed good prediction for the neuroblocking activities because of low average residual (CoMFA: 0.08, CoMSIA: 0.11) and PRESS (CoMFA: 0.32 & CoMSIA; 0.27) of training set, indicating good predictivity of the model. The $r^2_{cv.}$ (or q^2) values of the two optmized models were 0.707 and 0.715, respectively. For further validation of the predictive power of the two models, observed (*Obs*.log(1/BC)) and predicted activities (*Pred*.log(1/BC)) of five compounds in the test set are shown in Table 4. The two optimized models (CoMFA A5 & CoMSIA A3) can suggest good prediction for neuroblocking activities of the test set. The average values of deviation by the two models were 0.09 and 0.12, respectively.

Comparison of Predicted and Experimental. Predicted and experimental activities are shown in Table 1. To evaluate the CoMFA model as an example, a plot between observed activities and predicted activities of the training set molecules showed good linearity (*Pred*.log(1/BC)=0.972 *Obs*.log(1/BC) + 0.104, n = 16, s = 0.147, F = 297.554, r^2 = 0.955 & q^2 = 0.940) as depicted Figure 3. Additionally, predicted versus experimental activities for the test set are shown within the correlation plot of the CoMFA analysis for the neuroblocking activity. As indicated in CoMFA, a CoMSIA plots between observed activities and predicted activities of the training set molecules show good linearity (*Pred*.log(1/BC) = 0.961*Obs*.log(1/BC) + 0.810, n = 16, s = 0.137, F = 338.142, r^2 = 0.960 & q^2 = 0.956, not shown).

CoMFA Models for Activities. The statistical results of 10 CoMFA models (A1-A5 & F1-F5) with atom based fit and field fit alignment obtained from the combination of five fields (Standard, Indicator, Standard + Indicator, Standard + Hydrogen bond & Standard + Indicator + Hydrogen bond) are listed in Table 2. However, there are some important physicochemical parameters of insecticides whose hydrophobicity logP (0.00-5.50), dipole moment (μ = 1.20-10.20 debye), surface area (190-384 Å^2), and molar refractivity (MR = 48.0-121.0 Cm^3/mol), respectively, which are known to be taken up through the recent our study.[29] Particularly, to

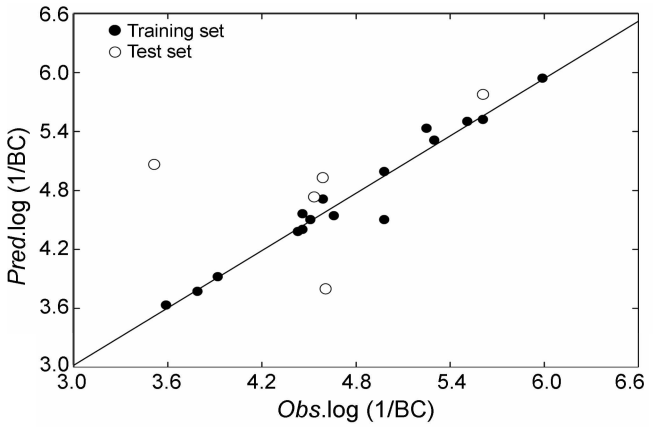

Figure 3. Relationships between observed neuroblocking activities, *Obs*.log(1/BC) and predicted neuroblocking activities, *Pred*.log(1/BC) by CoMFA model A5. (For training set; *Pred*.log(1/BC) = 0.972*Obs*.log(1/BC) + 0.104, n = 16, s = 0.147, F = 297.554, r^2 = 0.955 & q^2 = 0.940).

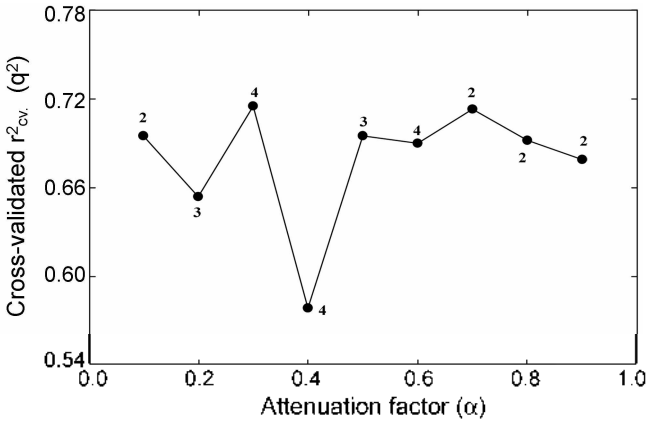

Figure 4. Variation of $r_{cv.}^2$ (or q^2) upon changing the attenuation factor, a used in the distance dependence between the probe atom and the atoms of the molecules in CoMSIA A3 model.

account for the hydrophobic properties, ClogP hydrophobicity (HINT) terms of molecules was included in the analysis as additional descriptor.[23] Inclusion of these descriptors improved the statistical significance of the model. These descriptors may influence this type of activity, an important parameter to explain relationship between substrates and receptor. The optimized A5 model shows that leave-one-out cross-validated value ($r^2_{cv.}$ or q^2) is 0.707 and non cross-validated conventional value ($r^2_{ncv.}$) is 0.986, which can suggest good prediction for neuroblocking activities of the training set. The contribution of steric, electrostatic and hydrophobic field was 76.4%, 21.9% and 1.7%, respectively. It suggests that steric bulk and electropositive nature of a compound is essential for high activity.

CoMSIA Models for Activities. The CoMSIA analysis with the same training set was performed. The statistical results of CoMSIA models (A1-A5 & F1-F5) with atom based fit and field fit alignment obtained from the combination of five fields (Steric, Electrostatic, Hydrophobicity, H-bond donor & H-bond acceptor) and the 10 models are listed in Table 3. It was found that CoMSIA A3 model gave best results (q^2 = 0.715 and $r^2_{ncv.}$ = 0.961). The contribution of steric, H-bond donor and H-bond acceptor fields was 68.2%, 0.8% and 31.0%, respectively. Therefore, this suggests that bulk and H-bond acceptor nature of a compound may offer favorable steric interactions at the active site from the contour maps with the two models. In order to determine an appropriate attenuation factor (α), a Gaussian-type distance dependence function is applied. In preliminary parameter study, it was calibrated within the range from 0.1 to 0.9, and q^2 values were computed each time. Figure 4 represents the most proper attenuation factor, α value that is distance dependent between probe atoms and atoms in the molecule in CoMSIA model. From the relationships between q^2 and α values, our systematic parameter study on attenuation factor shows that α = 0.3 is optimum for these data sets. From the results of 3D-QSAR analyses, the CoMFA and CoMSIA models from the atom based fit alignment (A) were better than that from the field fit alignment (F).

Contour plots of CoMFA and CoMSIA. The results of CoMFA and CoMSIA analyses were graphically interpreted by field contour plots and the coefficient contour maps using the field type 'StDev*Coeff' were generated as Figures 5 and 6, respectively. At first, Figure 5 shows a contour plots with the optimized CoMFA model A5. In the steric and electrostatic contour plot (shown in left), there is a large green and blue contour at X-substituent. The plots indicate that both the steric and electrostatic regions mainly are in the vicinity of the X-substituent. Green color denotes the contribution to steric and blue color denotes the contribution to positive charge. A positive electrostatic potential region, favorable to activity, and overlaps the steric region around the X-substituent. According to 2D-QSAR study of the X-substituents at 5-position on the pyridine ring, the greater the electron-releasing resonance effect (-R), higher the activity. However, introduction of sizable and alkoxy substituents were unfavorable.[19] HINT contour plot (right) also shows cyan contour at the same site. Cyan color denotes the contribution to the hydrophilicity. It means that introducing steric bulky, positive charge and hydrophilic substituent as

Table 4. Observed neuroblocking activities, Obs.log(1/BC) and predicted activities of imidacloprid analogues in the test set using 3D-QSAR models

No.	Sub. (X)	Obs.	CoMFA		CoMSIA	
			Pred.	Dev.	Pred.	Dev.
1	H	5.70	5.50	0.20	5.79	−0.09
8	*n*-C_3H_7O	4.56	4.58	−0.02	4.65	−0.09
10	*n*-C_4H_9O	4.58	3.66	0.92	3.83	0.75
13	C_2H_5	4.66	4.88	−0.22	4.85	−0.19
20	NO_2	3.60	5.05	−1.45	4.42	−0.82
	ARTS			0.09		0.12

Pred.; predicted values by the optimized CoMFA model (A5) in Table 2 and CoMSIA model (A3) in Table 3, Dev.; different between observed and predicted value, ARTS; average residual of test set.

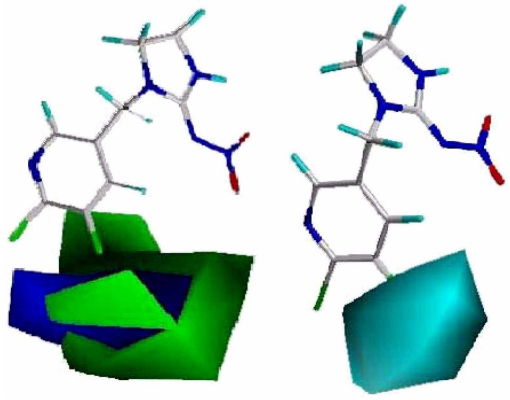

Figure 5. The contour plot of the CoMFA for the neuroblocking activities. left: the steric and electrostatic fields & right: CoMFA-HINT contour plot for hydrophilic field (stdev*coeff). The most active compound (**2**) is shown in capped sticks. (contour levels: favor; 80% & disfavor; 20%).

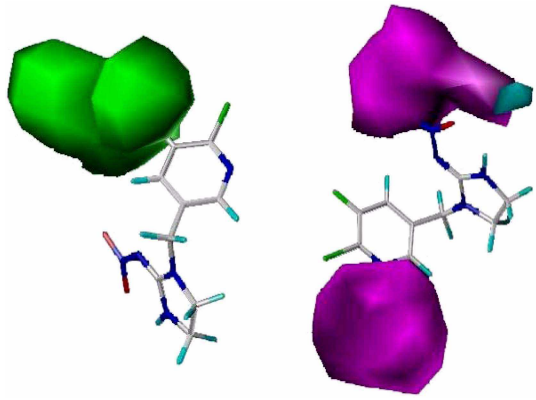

Figure 6. The contour plot of the CoMSIA for the neuroblocking activities. Right: for the steric field & Left: H-bond donor and H-bond acceptor fields (stdev*coeff). the most active compound (**2**) is shown in capped sticks. (contour levels: favor; 80% & disfavor; 20%).

X-substituent improves the neuroblocking activities.

The contour plots with optimized CoMSIA model (A3) are illustrated in Figure 6. Green color denotes the contribution to the steric field and magenta color denotes the contribution to H-bond acceptor. CoMSIA steric contour plots (left) show similar tendency to that of CoMFA.[13c] H-bond donor and acceptor contour plot (right) shows that H-bond acceptor region (magenta), favorable to activity, located at nitrogen atom on the pyridine ring and nitro group on the imidazolidine ring. But H-bond donor[30] favor region (cyan) located at one of the oxygen atom on nitro group. Based on these findings, the 3D-QSARs between X-substituents of imidacloprid analogues and their neuroblocking activities may be useful for designing better neuroblocking insecticides development.

Conclusion

The 3D-QSAR studies were performed for neuroblocking of imidacloprid analogues using CoMFA and CoMSIA methodology and highly predictive 3D-QSAR models were generated for neuroblocking for the treatment of imidacloprid analogues. The optimized CoMFA model (A5: $r^2_{cv.}$ = 0.707 & $r^2_{ncv.}$ = 0.986) and CoMSIA model (A3: $r^2_{cv.}$ = 0.715 & $r^2_{ncv.}$ = 0.961) for neuroblocking activity exhibited a good correlation. The contribution of steric, H-bond donor and H-bond acceptor fields was 68.2%, 0.8% and 31.0%, respectively. The two models generated from the atom based fit alignment (A) were better than that from the field fit alignment (F). From the contour plots with the two models, introducing steric bulky, positive charge and hydrophilic group as X-substituent improves the neuroblocking activities. And H-bond acceptor region which is favorable to activity, located at nitrogen atom on the pyridine ring and nitro group on the imidazolidine ring. Therefore, the models indicate the significant correlation of steric and H-bond acceptor fields with neuroblocking activities of imidacloprid analogues.

Acknowledgement. This work was supported by a grant (No. R11-2002-100-03005) from ERC program of the Korea Science and Engineering Foundation (KOSEF).

References

1. The British Crop Protection Council, In *The Pesticide Manual*, 13th ed.; The Royal Society of Chemistry; Tomlin, C. D. Ed.; Hampshire, UK. 2003; p 562.
2. (a) Hollingworth, R. M. In *Agrochemical Discovery; Insect, Weed, and Fungal Control*; Baker, D. R., Umetsu, N. K., Eds.; ACS Symposium Series 774; Washington DC, 2001; p 238. (b) Kagabu, S. *Rev. Toxicol.* **1997**, *1*, 75.
3. Levin, E. D.; Simon, B. B. *Psychopharmacology* (Berlin) **1998**, *138*, 217.
4. Simms, L. C.; Ester, A.; Wilson, M. J. *Crop. Protection* **2006**, *25*, 549.
5. Byrne, F. J.; Toscano, N. C. *Crop. Protection* **2006**, *25*, 831.
6. Capowiez, Y.; Berard, A. *Ecotoxicol. Environ. Saf.* **2006**, *64*, 198.
7. (a) Kim, H. J.; Shelver, W. L.; Li, Q. X. *Anal. Chim. Acta* **2004**, *509*, 111. (b) Watanabe, E.; Eun, H.; Baba, K.; Arao, T.; Ishi, Y.; Endo, S.; Ueji, M. *J. Agric. Food Chem.* **2004**, *52*, 2756. (c) Zhang, N.; Tomizawa, M.; Casida, J. E. *Neurosci. Lett.* **2004**, *371*, 56.
8. Guez, D.; Belzunces, L. P.; Maleszka, R. *Pharm. Biochem. Behav.* **2003**, *75*, 217.
9. (a) Jepson, J. E. C.; Brown, L. A.; Sattle, D. B. *Invert. Neurosci.* **2006**, *6*, 33. (b) Ihara, M.; Brown, L. A.; Ishida, C.; Okuda, H.; Sattelle, D. B.; Matsuda, K. *J. Pestic. Sci.* **2006**, *3*, 35. (c) Kagabu, S.; Kato, C.; Nishimura, K. *J. Pestic. Sci.* **2004**, *29*, 376.
10. Decourtye, A.; Devillers, J.; Cluzeau, S.; Charreton, M.; Pham-Delegue, M. H. *Ecotoxi. Environ. Saf.* **2004**, *57*, 410.
11. Rancan, M.; Sabatini, A. G.; Achilli, G.; Galletti, G. C. *Anal. Chim. Acta* **2006**, *555*, 20.
12. Karabay, N. U.; Oguz, M. G. *Gen. Mol. Res.* **2005**, *4*, 653.
13. (a) Matsuo, H.; Tomizawa, M.; Yamamoto, I. *Arch. Insect Biochem. Physiol.* **1998**, *37*, 17. (b) Yamamoto, I.; Tomizawa, M.; Saito, T.; Miyamoto, T.; Walcott, E. C.; Sumikawa, K. *Arch. Insect. Biochem. Physiol.* **1998**, *37*, 24. (c) Okazawa, A.; Akamatsu, M.; Ohaka, A.; Nishiwaki, H.; Cho, W. J.; Nakagawa, Y.; Nishimura, K.; Ueno, T. *Pestic. Sci.* **1998**, *54*, 134. (d) Nishiwaki, H.; Nakagawa, Y.; Takeda, D. Y.; Okazawa, A.; Akamatsu, M.; Miyagawa, H.; Ueno, T.; Nishimura, K. *Pest. Manag. Sci.* **2000**, *56*, 875. (e) Kagabu, S.; Ito, N.; Imai, R.; Hieta, Y.; Nishimura, K. *J. Pestic. Sci.* **2005**, *30*, 409.

14. Nicolotti, O.; Altomare, C.; Pellegrini-Calace, M.; Carotti, A. *Curr. Topics Med. Chem.* **2004**, *4*, 335.
15. Sung, N. D.; Yu, S. J.; Kang, M. S. *Agri. Chem. & Biotechnol.* **1997**, *40*, 53.
16. (a) Cramer, R. D.; Patterson, D. E.; Bunce, J. D. *J. Am. Chem. Soc.* **1988**, *110*, 5959. (b) Cramer, R. D.; Bunce, J. D.; Patterson, D. E. *Quant. Struct. Act. Relat.* **1988**, *7*, 18.
17. (a) Klebe, G.; Abraham, U.; Mietzner, T. *J. Med. Chem.* **1994**, *37*, 4130. (b) Kebe, G.; Abraham, U. *J. Comput. Aided Mol. Des.* **1999**, *13*, 1.
18. Folkers, G.; Merz, A.; Rognam, D. In *3D-QSAR in Drug Design: Theory, Methods and Applications*; Kubinyi, H., Ed.; ESCOM Science Publishers, B. V.: 1993; p 583.
19. Nishimura, K.; Kiriyama, K.; Kagabu, S. *J. Pestic. Sci.* **2006**, *31*, 110.
20. *Sybyl Molecular Modeling and QSAR Software on CD-Rom (Ver. 7.1)*, Theory Manual; Tripos Inc.: St. Louis, U.S.A., 2005.
21. Purcell, W. P.; Singer, J. A. *J. Chem. Eng. Data* **1967**, *122*, 235.
22. Kerr, R. *Biophys. J.* **1994**, *67*, 1501.
23. Marshall, G. R.; Barry, C. D.; Bosshard, H. E.; Dammkoehler, R. A.; Dunn, D. A. In *Computerassisted Drug Design*: Olsen, E. C.; Christoffersen, R. E., Eds.; ACS: Washington D.C., 1979; p 205.
24. Clark, M.; Cramer III, R. D.; Jones, D. M.; Patterson, D. E.; Simerroth, P. E. *Tetrahedron Comput. Methodol.* **1990**, *3*, 47.
25. Kellogg, G. E.; Semus, S. F.; Abraham, D. J. *J. Comp.-Aided Mol. Design* **1991**, *5*, 545.
26. (a) Lindgren, F.; Geladi, P.; Rannar, S.; Wold, S. *J. Chemometrics* **1994**, *8*, 349. (b) Lindgren, F.; Geladi, P.; Berglund, A.; Sjostrom, M.; Wold, S.; Chemometrics, J. *J. Chemometrics* **1995**, *9*, 331.
27. (a) Klebe, G. In *3D-QSAR Drug Design, Theory, Methods and Applications*; Kubinyi, H., Ed.; ESCOM: Leiden, 1993; p 173. (b) Klebe, G.; Abraham, U. *J. Comput. Aid. Mol. Des.* **1999**, *13*, 1.
28. Klebe, G.; Abraham, U.; Mietzner, T. *J. Med. Chem.* **1994**, *37*, 4130.
29. Sung, N. D.; Song, S. S. *J. Korean Soc. Agric. Chem. Biotechnol.* **2003**, *46*, 280.
30. (a) Etter, M. C. *Acc. Chem. Res.* **1990**, *23*, 120. (b) Taylor, B.; Kennard, O. *Acc. Chem. Res.* **1984**, *17*, 320.